DALTON
FULL PAPER

A synthetic and structural study of the formation of cyclic $[(RP)_nE]^-$ anions and Zintl compounds using $E(NMe_2)_3$ (E = As, Sb)

Alan Bashall,[a] Michael A. Beswick,*[b] Nick Choi,[a] Alexander D. Hopkins,[b] Sara J. Kidd,[b] Yvonne G. Lawson,[b] Marta E. G. Mosquera,[b] Mary McPartlin,[a] Paul R. Raithby,[b] Andrew A. E. H. Wheatley,[b] Jody A. Wood[b] and Dominic S. Wright*[b]

[a] *School of Chemistry, University of North London, London, UK N7 8DB*
[b] *Chemistry Department, University of Cambridge, Lensfield Road, Cambridge, UK CB2 1EW. E-mail: dsw1000@cus.cam.ac.uk*

Received 27th October 1999, Accepted 15th December 1999

The low-temperature reactions of aliphatic primary phosphines and phosphides with $E(NMe_2)_3$ (E = As, Sb) give cyclic anions of the type $[(RP)_nE]^-$. At higher temperatures Zintl compounds containing E_7^{3-} anions are generated. In contrast, related reactions using aryl phosphines lead to the direct formation of Zintl compounds even at low temperature. The reactions of aliphatic and aryl arsines follow a similar pattern to that of the corresponding phosphines. The syntheses and X-ray structures of several complexes containing $[(RP)_nE]^-$ (n = 3 or 4) and E_7^{3-} anions are reported.

Introduction

In recent years a variety of synthetic strategies have been developed to produce cage compounds containing anionic Group 15 and 16 element/imido ligands (such as the isoelectronic $[Sb(NR)_3]^{3-}$ trianion[1] and $[S(NR)_3]^{2-}$ dianion[2]). Our approach has involved the reactions of metallated primary amines (RNHM; M = Li–Cs) with a range of dimethylamido Group 15 reagents.[3] Such step-wise metallation has proved highly versatile in the construction of a number of imido ligand frameworks with different functionalities (Chart 1). These anions have an interesting coordination chemistry. Generally, complete exchange of the alkali metal counter ions occurs on addition of main group and transition metal salts, yielding new heterometallic cages in which the imido Group 15 ligand frameworks are preserved.[4]

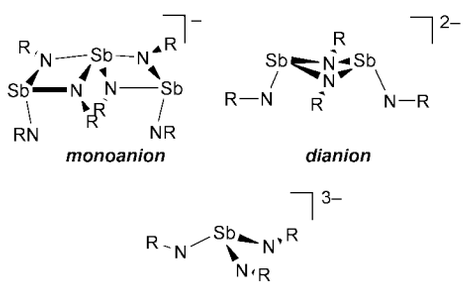

Chart 1

In further studies we aimed to extend the work on the imido ligands to the phosphorus counterparts in order to provide more suitable ligands for the coordination of softer (particularly low oxidation state) transition metals. The heterometallic Sb(III)/Li cage $[\{Sb(PCy)_3\}_2Li_6{\cdot}6Me_2NH]{\cdot}2$(toluene) (containing the $[Sb(PCy)_3]^{3-}$ trianion; Cy = C_6H_{11}) is readily prepared by the reaction of CyPHLi with $Sb(NMe_2)_3$ (3 : 1 equiv).[5] However, a surprising finding is that this complex (in contrast to the thermally stable imido analogue $[\{Sb(NCy)_3\}_2Li_6{\cdot}2Me_2NH]$) readily decomposes in solution at 30–40 °C to give the Zintl compound $[Sb_7Li_3{\cdot}6Me_2NH]$ in almost quantitative yield.[6] The isolation of *cyclo*-$[CyP]_4$ from this reaction indicates that the formation of P–P bonds provides the crucial thermodynamic driving force.[6] The importance of this alloy-forming process is that it furnishes a single-source approach to photoemissive alkali metal antimonate films from solution.[7]

We recently communicated further investigations of the reactions of phosphines (RPH_2) and metallated primary phosphines (RPHM) with $E(NMe_2)_3$ (E = As, Sb), showing that heterocyclic $[(RP)_nE]^-$ anions generated in these reactions are likely intermediates in the formation of the Zintl compounds ultimately produced.[8] We report here a full account of this work. In addition to $[\{(CyP)_4Sb\}Na{\cdot}Me_2NH{\cdot}TMEDA]_2$ (**1**) and $[\{(^tBuP)_3As\}Li{\cdot}thf{\cdot}TMEDA]$ (**2**), details of which were reported earlier,[8] we report here the syntheses and X-ray structures of the heterocyclic anion complexes $[\{(^tBuP)_3As\}Li{\cdot}TMEDA]_2{\cdot}TMEDA$ (**3**) (TMEDA = $\{CH_2CH_2\}_2NMe$), $[\{(^tBuP)_3As\}Li{\cdot}2DABCO{\cdot}thf]$ (**4**) (DABCO = $N\{CH_2CH_2\}_3N$) and $[\{(1\text{-}AdP)_3As\}Li{\cdot}thf{\cdot}TMEDA]{\cdot}0.5$(toluene) [**5**·0.5(toluene)] (Ad = adamantyl), and the Zintl compounds $[Sb_7Na_3{\cdot}3TMEDA{\cdot}3thf]$ (**6**) and $[As_7Li_3{\cdot}3TMEDA]{\cdot}1.5$(toluene) [**7**·1.5(toluene)]. A novel synthesis of the bicylic compound $[(^tBuAs)_3As]_2$ (**8**) is also reported.

Results and discussion

The syntheses of $[\{(CyP)_4Sb\}Na{\cdot}Me_2NH{\cdot}TMEDA]_2$ (**1**) (Fig. 1), from the 1 : 1 : 1 reaction of $CyPH_2$ with $Sb(NMe_2)_3$ followed by the addition of CyPHNa, and of $[\{(^tBuP)_3As\}Li{\cdot}thf{\cdot}TMEDA]$ (**2**) (Fig. 2), from the 1 : 3 reaction of $As(NMe_2)_3$ with ^{t}BuPHLi, provide extremely simple one-pot approaches to heterocyclic anions of the type $[(RP)_nE]^-$. In the current study we aimed not only to confirm the generality of this route and to investigate the coordination characteristics of the $[(RP)_nE]^-$ anions, but also to assess the affects in particular of changing the stoichiometry of the reactions employed, the substituents (R) and Group 15 elements (E) present. These issues are key to the future development of these anions as novel ligands to a variety of transition and main group metals.

Mesityl phosphine [2,4,6-$Me_3C_6H_2PH_2$ = $MesPH_2$],[9] *tert*-butyl phosphine ($^tBuPH_2$),[10] 1-adamantyl phosphine ($C_{10}H_{15}PH_2$ = 1-$AdPH_2$),[11] phenyl arsine ($PhAsH_2$)[12] and *tert*-butyl arsine ($^tBuAsH_2$)[13] were chosen as reactants since they are

readily prepared by literature procedures and provide the opportunity to assess the effects of varying the steric demands and electronic character of the organic substituents (R) and the Group 15 elements (E) on the products formed in these reactions. The reactions of the phosphines and their metallates which were carried out in this study with $As(NMe_2)_3$ and $Sb(NMe_2)_3$ are summarised in Scheme 1. We had already established in earlier work that heterobimetallic Sb(III)/alkali metal imido complexes of the type $[\{Sb_2(NR)_4\}_2M_4]$ (where M = Li or Na) can be prepared by the reaction of $Sb(NMe_2)_3$ with primary amines (RNH_2) followed by reaction of the dimers $[(Me_2N)Sb(\mu\text{-}NR)]_2$ produced with the metallated primary amine (RNHM). The reaction of $Sb(NMe_2)_3$ with $CyPH_2$ followed by the addition of CyPHNa was carried out in our preliminary work in an attempt to prepare an analogous heterobimetallic Sb(III)/Na phosphide complex $[\{Sb_2(PCy)_4\}_2Na_4]$. The isolation of $[\{(CyP)_4Sb\}Na\cdot Me_2NH\cdot TMEDA]_2$ (**1**) from this reaction at or below 0 °C in the presence of TMEDA was therefore completely unexpected. This result, combined with the formation of $[\{(^tBuP)_3As\}Li\cdot thf\cdot TMEDA]$ (**2**) from the 1:3 reaction of $As(NMe_2)_3$ with ^{t}BuPHLi, suggested that the stoichiometry may have a direct bearing on the size of the heterocyclic anion formed. Unfortunately, repeated attempts to test this hypothesis by preparing the $[(^tBuP)_3Sb]^-$ anion, from the reaction of ^{t}BuPHLi (3 equiv.) and $Sb(NMe_2)_3$ (1 equiv.) in the presence of TMEDA, resulted only in the formation of $[Sb_7Li_3\cdot 3TMEDA]$.[6] However, the reaction of $As(NMe_2)_3$ with ^{t}BuPH$_2$ followed by the addition of [^{t}BuPHLi] in the presence of TMEDA (a reaction analogous to that producing the five-membered $[\{CyP\}_4Sb]^-$ anion in **1**) gives $[\{(^tBuP)_3As\}Li\cdot TMEDA]_2\cdot TMEDA$ (**3**) (containing the same $[(^tBuP)_3As]^-$ anion as that present in **2**). This result provides a strong indication that the stoichiometry of the reaction employed has no effect on the nature of the product. We suggest that the Group 15 element present (As or Sb) probably has the primary role in dictating the ring size of the anion. In view of the later structural characterisation of **3** (containing a Li–TMEDA–Li bridge), the reaction of $As(NMe_2)_3$ with [^{t}BuPHLi] (1:3 equiv) in DABCO (1 equiv.)–toluene was carried out in an attempt to obtain a cyclic or polymeric Li–DABCO–Li bridged complex, $[\{(^tBuP)_3As\}Li\cdot DABCO]$. However, thf was required to solubilise the product initially formed and only $[\{(^tBuP)_3As\}Li\cdot 2DABCO\cdot thf]$ (**4**) could be isolated in this case. A similar $[(PR)_3As]^-$ anion $[\{(1\text{-}AdP)_3As\}Li\cdot thf\cdot TMEDA]\cdot 0.5(toluene)$ [**5**·0.5(toluene)] to that present in **2** and **3** is also formed in the reaction of $As(NMe_2)_3$ with [1-AdPHLi] (1:3 equiv) in TMEDA (1 equiv.)–thf–toluene.

The ^{31}P NMR spectra of complexes **2**–**5** are particularly diagnostic, the central P atoms and As-bonded P atoms of the $[(RP)_3As]^-$ anions appearing as a well separated triplet and doublet [δ 7.9 and −74.5 in **2** (respectively),[8] 7.8 and −75.1 in **3**, 5.0 and −73.6 in **4** and −11.9 and −89.9 in **5**·0.5(toluene) (relative to 80% H_3PO_4–D_2O)], with coupling constants ($^1J_{PP}$) which are typical of other compounds containing single P–P

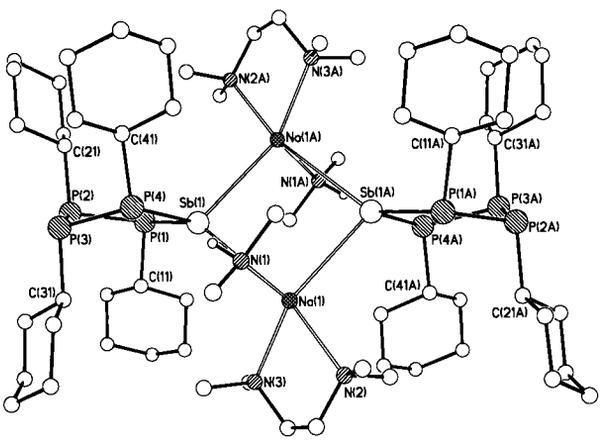

Fig. 1 An illustration of the centrosymmetric structure of $[\{(CyP)_4Sb\}Na\cdot Me_2NH\cdot TMEDA]_2$ (**1**). Atom labels ending in A denote atoms at $-x+2, -y+1, -z$.

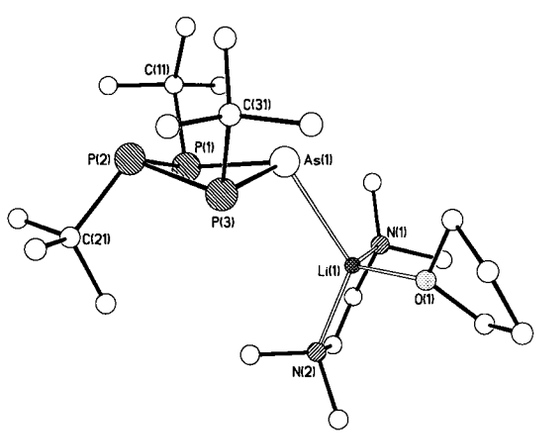

Fig. 2 Structure of molecules of $[\{(^tBuP)_3As\}Li\cdot thf\cdot TMEDA]$ (**2**). H-atoms and lattice-bound toluene molecules are omitted for clarity. Selected bond lengths and angles are listed in Table 2.

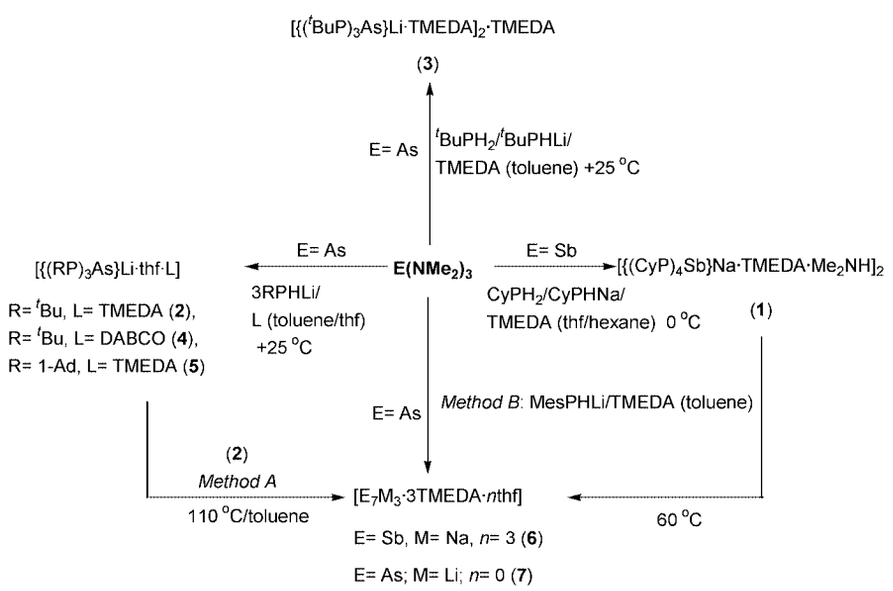

Scheme 1 Complex **2** is isolated as its toluene solvate [**2**·0.5(toluene)]. Method A gives the toluene solvate **7**·1.5(toluene) (see Experimental Section).

Table 1 Crystal data and structural refinements of [{(^{t}BuP)$_3$As}Li·TMEDA]$_2$·TMEDA (**3**), [{(^{t}BuP)$_3$As}Li·2DABCO·thf] (**4**), [{(1-AdP)$_3$As}-Li·thf·TMEDA]·0.5toluene (**5**), [Sb_7Na_3·3TMEDA·3thf] (**6**) and [As_7Li_3·3TMEDA]·1.5(toluene) [**7**·1.5(toluene)]

Compound	**3**	**4**	**5**·0.5(toluene)	**6**	**7**·1.5(toluene)
Formula wt.	520.42	642.56	814.81	940.05	1032.08
Crystal system	Triclinic	Triclinic	Triclinic	Monoclinic	Monoclinic
Space group	$P\bar{1}$	$P\bar{1}$	$P\bar{1}$	$P2(1)/m$	$P2(1)/c$
a/Å	9.218(5)	11.651(2)	12.518(6)	10.207(3)	12.1225(5)
b/Å	11.182(6)	12.638(2)	17.347(4)	22.101(6)	11.6572(8)
c/Å	15.967(8)	13.991(3)	11.166(4)	11.719(3)	31.7097(8)
α/°	108.44(2)	71.11(3)	100.07(2)	—	—
β/°	90.46(2)	73.79(3)	112.31(3)	92.25(2)	91.618(5)
γ/°	108.01(2)	64.61(3)	79.90(3)	—	—
V/Å^3	1474.6(13)	1737.0(6)	2192.8(14)	2641.7(11)	4479.3(3)
Z	2	2	2	2	4
μ/mm^{-1}	1.327 (Mo-Kα)	1.142 (Mo-Kα)	0.918 (Mo-Kα)	3.581 (Cu-Kα)	6.134 (Cu-Kα)
T/K	180(2)	180(2)	180(2)	223(2)	203(2)
θ/°	3.57–22.50	1.56–27.48	2.66–27.51	1.97–21.00	2.79–20.99
Reflections collected	4457	11462	10544	3779	5884
Independent reflections (R_{int})	3823 (0.063)	7903 (0.027)	10082 (0.028)	2935 (0.098)	4340 (0.031)
R indices [$(F > 4\sigma(F)$][31]	$R1 = 0.044$, $WR2 = 0.092$	$R1 = 0.036$, $WR2 = 0.091$	$R1 = 0.052$, $WR2 = 0.120$	$R1 = 0.086$, $WR2 = 0.206$	$R1 = 0.047$, $WR2 = 0.118$
R indices (all data)	$R1 = 0.063$, $WR2 = 0.102$	$R1 = 0.056$, $WR2 = 0.117$	$R1 = 0.076$, $WR2 = 0.133$	$R1 = 0.155$, $WR2 = 0.230$	$R1 = 0.063$, $WR2 = 0.137$

bonds (176.0 to 181.7 Hz in **2**–**5**).[14] The lower chemical shift for the As-bonded P centres is symptomatic of the concentration of negative charge on the As atoms of the anions. Owing to the thermal instability of [{(CyP)$_4$Sb}Na·Me$_2$NH·TMEDA]$_2$ (**1**) and its extreme air and moisture sensitivity, we had previously not been able to obtain satisfactory ^{31}P NMR spectra of isolated samples of the complex.[8] However, we have now been able to do so using freshly prepared samples of **1** separated from the reaction solution by cannula transfer (all apparatus being kept at *ca.* 0 °C). Although such samples are contaminated with significant amounts of [CyP]$_4$ (s, δ −67.0) and CyPH$_2$ (t, δ −112.1) (present in the reaction mixture and/or by trace hydrolysis), the identity of **1** in solution is confirmed by the observation of one dominant ring isomer, as an AA′BB′ pattern [the terminal P atoms [P(1,4)] at δ 19.7 and the central P atoms [P(2,3)] at δ 59.5 (relative to 85% H_3PO_4/D_2O)].[15a] This pattern is extremely similar to that previously observed for the predominant "*threo*, *dl*, *threo*" chain isomer of [(^{t}BuP)$_4$H$_2$][15b] [the same (*cis*, *trans*, *cis*, *trans*) conformation of Cy groups as observed in the [(CyP)$_4$Sb]$^-$ anions of **1** in the solid state (Fig. 1)], although the ^{31}P chemical shifts for **1** are at higher values [[(^{t}BuP)$_4$H$_2$]; P(1,4) δ −50.3, P(1,2) δ −29.8, relative to the same external standard]. Simulation of the spectrum[15c] gives the coupling constants as $J_{P(1)-P(2)} = -333.6$ Hz, $J_{P(1,2)-P(3,4)} = 12.8$ Hz, $J_{P(2)-P(3)} = -340.9$ Hz and $J_{P(1)-P(4)} = 3.0$ Hz (*cf.* −218.6, −6.8, −342.4, 22.1 Hz for the corresponding values in [(^{t}BuP)$_4$H$_2$][15b]).

If the reaction producing **1** is heated briefly to *ca.* 60 °C then the Zintl compound [Sb_7Na_3·3TMEDA·3thf] (**6**) is isolated. Highest yields of **6** are obtained for more concentrated reaction mixtures, with almost quantitative yields of the complex being formed if the quantity of solvent is halved. A similar result is observed if the reactions producing **2** and **3** are carried out at elevated temperatures for prolonged periods, reaction times of *ca.* 48 h at reflux producing the Zintl compound [As_7Li_3·3 TMEDA] (**7**) as its toluene solvate [**7**·1.5(toluene)] in near quantitative yield in the case of **2** (see Method A, Experimental section). The lower thermal stability of the [(CyP)$_4$Sb]$^-$ anion of **1** is presumably a consequence of the presence of weaker P–Sb bonds and of the elimination of the more thermodynamically stable (*i.e.*, less strained) *cyclo*-[CyP]$_4$ byproduct in the formation of the Zintl compound. Complex **7** is far more easily prepared by the 1:3 reaction of As(NMe$_2$)$_3$ with [MesPHLi] at room temperature (see Method B, Experimental section). In this case **7** is formed after a reaction time of 1 h. This outcome suggests that for the isolation of stable cyclic anions (like those of **2**–**5**) aliphatic groups should be employed, since otherwise direct formation of Zintl compounds occurs.

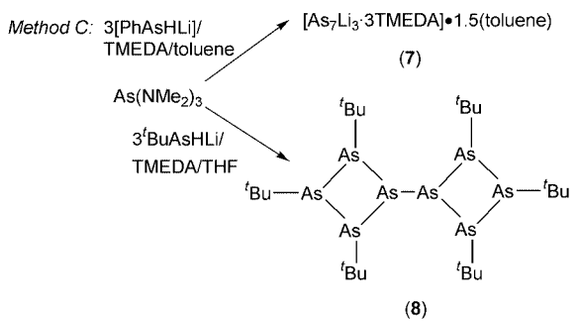

Scheme 2

Reactions involving arsines (Scheme 2) follow a similar trend to that observed for the phosphines described above, although there appears to be an even greater tendency for the formation of coupled products. The reaction of As(NMe$_2$)$_3$ with the lithiated aryl arsine [PhAsHLi] (1:3 equiv) in the presence of TMEDA also generates **7** (Method C, Experimental section). Whereas the reaction of As(NMe$_2$)$_3$ with the lithiated aliphatic arsine [^{t}BuAsHLi] gives the bicyclic compound [{^{t}BuAs}$_3$As]$_2$ (**8**) in low yield, which has previously been prepared by the coupling reaction of ^{t}BuAsCl$_2$ with AsCl$_3$ and Mg metal.[16]

Low-temperature X-ray studies of compounds **1**–**7** have been carried out and we have previously reported details of the structures of **1** and **2**,[8] so here we give a full report only for the structures of **3**–**7**. Driess and co-workers have given a brief preliminary report[17] of the unsolvated complex [As_7Li_3·3TMEDA] **7**, which was found to have disordering of the TMEDA ligands; in the toluene solvate **7**·1.5(toluene), reported here, there is no disordering of the Zintl complex and the structure is well defined. Crystal data and refinement parameters for crystals **3**–**7** are given in Table 1. Table 2 compares selected bond lengths and angles for **3**, **4** and **5** with those previously reported for **2**. Selected bond lengths and angles for **6** and **7** are given in Tables 3 and 4 respectively.

The low-temperature X-ray structures of complexes **3** (Fig. 3), **4** (Fig. 4) and **5**·0.5(toluene) (Fig. 5) confirm that, like complex **2**, all contain cyclic [(RP)$_3$As]$^-$ anions. The centrosymmetric dimer structure of complex **3** is composed of two crystallographically identical [(^{t}BuP)$_3$AsLi·TMEDA] monomer units in which the Li$^+$ cation is coordinated in a conventional chelating manner by the TMEDA ligand (Fig. 3). These units

Table 2 Selected bond lengths (Å) and bond angles (°) for [{('BuP)$_3$AsLi·thf·TMEDA] (**2**), [{('BuP)$_3$As}Li·TMEDA]$_2$·TMEDA (**3**), [{('BuP)$_3$As}-Li·2DABCO·thf] (**4**), [{(1-AdP)$_3$As}Li·thf·TMEDA]·0.5(toluene) [**5**·0.5(toluene)]

	2	**3**	**4**	**5**·0.5(toluene)
P(1)–P(2)	2.203(4)	2.209(2)	2.210(1)	2.242(1)
P(2)–P(3)	2.198(4)	2.205(2)	2.212(1)	2.230(1)
P(1)–As(1)	2.333(4)	2.328(2)	2.335(1)	2.356(1)
P(3)–As(1)	2.324(3)	2.332(2)	2.336(1)	2.350(1)
C–P(1,2,3)	mean 1.90	mean 1.90	mean 1.90	mean 1.90
As(1)–Li(1)	2.62(2)	2.683(8)	2.702(4)	2.666(6)
Li(1)–N(ligand)	mean 2.10	mean 2.15	mean 2.07	mean 2.12
Li(1)–O(1)[N(3)][a]	1.92(2)	2.132(9)	1.963(4)	1.994(7)
P(1)–As(1)–P(3)	85.1(1)	85.08(6)	84.94(4)	83.67(4)
As(1)–P(1)–P(2)	88.2(1)	88.45(6)	88.84(4)	87.36(4)
As(1)–P(3)–P(2)	88.5(1)	88.43(7)	88.77(4)	87.79(5)
P(1)–P(2)–P(3)	91.4(2)	91.07(7)	91.02(4)	89.16(5)
External angles at P(1,2,3)	100.1(2)–107.8(2)	101.7(2)–106.3(2)	101.64(4)–107.32(8)	102.7(9)–106.2(1)
P(1)–As(1)–Li(1)	108.5(2)	108.8(2)	109.01(9)	103.8(1)
P(3)–As(1)–Li(1)	106.4(2)	107.3(2)	108.46(9)	100.1(1)
Angles at Li(1)	86.1(3)–127.5(3)	85.3(3)–127.2(3)	105.4(2)–117.7(2)	86.7(3)–127.9(3)
Puckering P$_3$As	27.6	28.1	28.0	36.5

[a] The value in parentheses is appropriate to complex **2**.

Table 3 Selected bond lengths (Å) and bond angles (°) for [Sb$_7$Na$_3$·3TMEDA·3thf] (**6**)

Sb(1)–Sb(21)	2.813(3)	Na(1)–Sb(21)	3.196(9)
Sb(1)–Sb(2)	2.793(2)	Na(1)–Sb(1)	3.563(9)
Sb(2)–Sb(3)	2.741(2)	Na(1)–O(1)	2.33(2)
Sb(21)–Sb(31)	2.743(4)	Na(1)–N(0,1)	mean 2.51
Sb(3)–Sb(3A)	2.865(4)	Na(2)–Sb(2)	3.240(8)
Sb(3)–Sb(31)	2.852(3)	Na(2)–N(2)	2.54(2)
Na(1)–Sb(2)	3.297(8)		
Sb(2)–Sb(1)–Sb(2A)	101.6(1)	Sb(2)–Sb(3)–Sb(31)	105.90(8)
Sb(2)–Sb(1)–Sb(21)	100.50(7)	Sb(21)–Sb(31)–Sb(3)	104.95(9)
Sb(1)–Sb(21)–Sb(31)	99.4(2)	Sb(2)–Na(2)–Sb(2A)	83.8(3)
Sb(1)–Sb(2)–Sb(3)	99.11(8)	Sb(2)–Na(1)–Sb(21)	83.2(2)
Sb(31)–Sb(3)–Sb(3A)	59.85(5)	Sb(1)–Na(1)–Sb(2)	47.7(2)
Sb(3)–Sb(31)–Sb(3A)	60.31(9)	Sb(1)–Na(1)–Sb(21)	48.7(2)
Sb(2)–Sb(3)–Sb(3A)	105.48(5)		

Table 4 Selected bond lengths (Å) and bond angles (°) for [As$_7$Li$_3$·3TMEDA]·1.5(toluene) [**7**·1.5(toluene)]

As(1)–As(2)	2.405(2)	Li(1)–As(2)	2.62(1)
As(1)–As(4)	2.399(2)	Li(1)–As(6)	2.64(2)
As(1)–As(6)	2.407(2)	Li(2)–As(2)	2.65(1)
As(2)–As(3)	2.372(2)	Li(2)–As(4)	2.61(2)
As(4)–As(5)	2.360(2)	Li(3)–As(4)	2.60(2)
As(6)–As(7)	2.368(2)	Li(3)–As(6)	2.66(2)
As(3)–As(5)	2.475(2)	Li(1)–N(mean)	2.11(2)
As(3)–As(7)	2.498(2)	Li(2)–N(mean)	2.10(2)
As(5)–As(7)	2.479(2)	Li(3)–N(mean)	2.09(2)
As(2)–As(1)–As(4)	100.41(6)	As(2)–As(3)–As(5)	104.73(6)
As(2)–As(1)–As(6)	101.72(6)	As(2)–As(3)–As(7)	102.82(6)
As(4)–As(1)–As(6)	101.19(5)	As(5)–As(3)–As(7)	59.80(5)
As(1)–As(2)–As(3)	99.54(6)	As(3)–As(5)–As(4)	105.04(6)
As(1)–As(4)–As(5)	99.76(6)	As(4)–As(5)–As(7)	104.94(6)
As(1)–As(6)–As(7)	99.15(5)	As(3)–As(5)–As(7)	60.54(5)
As(2)–Li(1)–As(6)	90.2(5)	As(6)–As(7)–As(3)	105.38(5)
As(2)–Li(1)–As(6)	89.0(4)	As(6)–As(7)–As(5)	105.41(5)
As(2)–Li(1)–As(6)	89.8(5)	As(3)–As(7)–As(5)	59.66(5)

are then linked together by a non-chelating, bridging TMEDA ligand. Although this pattern of aggregation is unusual, a similar arrangement to **3** has been observed in [Me$_3$SiLi·TMEDA]$_2$·TMEDA,[18] in which both chelating and non-chelating TMEDA ligands are present, and bridging TMEDA ligands have been observed in a number of other alkali metal complexes.[19] The comparatively large difference in the coordination environments of the Li$^+$ cations in **2**, **3** and **4** has no discernable effect on the geometries of their [('BuP)$_3$As]$^-$ anions

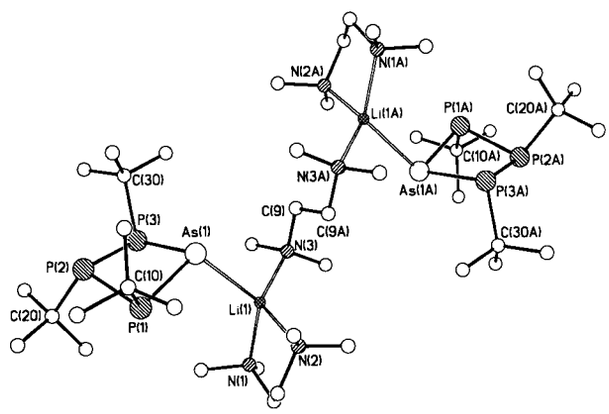

Fig. 3 The centrosymmetric dimer structure of [{('BuP)$_3$As}Li·TMEDA]$_2$·TMEDA (**3**). H-atoms and lattice-bound toluene molecules are omitted for clarity. Selected bond lengths and angles are listed in Table 2; atom labels ending in A denote atoms at $-x + 1$, $-y + 2$, $-z + 2$.

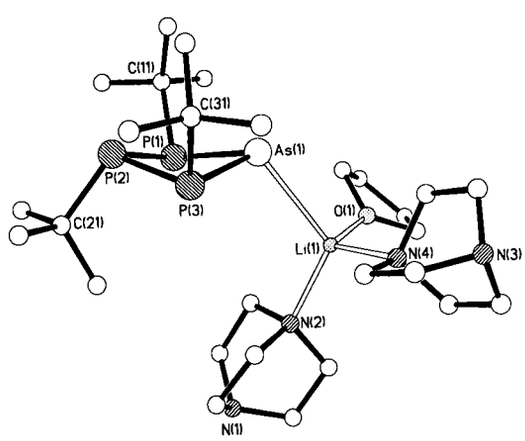

Fig. 4 Structure of molecules of [{('BuP)$_3$As}Li·2DABCO·thf] (**4**). H-atoms and lattice-bound toluene molecules are omitted for clarity. Selected bond lengths and angles are listed in Table 2.

and all of the key bond lengths and angles involved are identical to within crystallographic errors (the P–P bonds being *ca.* 2.20 Å, the P–As bonds being *ca.* 2.33 Å and the *endo*-P–P–P and P–As–P angles being *ca.* 91 and 85°, respectively, in these species). The only noticeable difference, resulting presumably from the greater steric congestion around the Li$^+$ cations in **3** and **4**, is the small elongation in the As–Li bond lengths

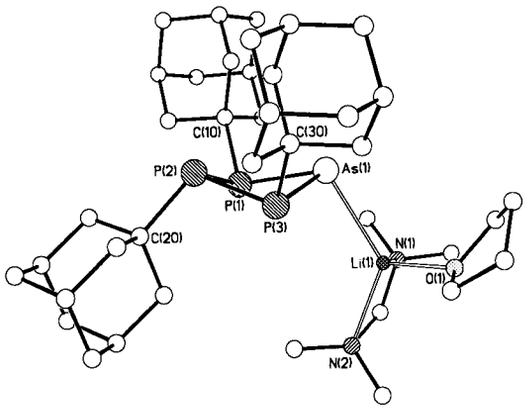

Fig. 5 Structure of molecules of [{(1-AdP)$_3$As}Li·thf·TMEDA]·0.5(toluene) [**5**·0.5(toluene)]. H-atoms and lattice-bound toluene molecules are omitted for clarity. Selected bond lengths and angles are listed in Table 2.

[2.683(8) and 2.702(4) Å, respectively] compared to that in **2** and **5** [2.62(2) and 2.666(6) Å]. The increase in the steric bulk of the organic substituents attached to P has only a small affect on the dimensions and geometry of the P_3As ring of **5**. In particular, both the P–As (mean 2.35 Å) and P–P (mean 2.24 Å) bond lengths in **5** are slightly longer than the corresponding bonds found in **2**, **3** and **4** (mean 2.33 and 2.21 Å, respectively, in these complexes) and there is also a small reduction in the *endo*-P–As–P angle [from *ca.* 85° in **2**–**4**, to 83.67(4)° in **5**].

Although a number of other As–Li bonded complexes containing various functional groups attached to As have been structurally characterised (the range of As–Li bonds in these species being 2.46–2.76 Å),[17,20] **2**–**5** are the first complexes of this type containing As–P bonds within the anion. Other cyclic As–P bonded species have been synthesised containing a range of stoichiometries and ring sizes, with the rings generally being supported by coordination to transition metal centres.[21] The closest relative of the $[(RP)_3As]^-$ ligands found in **2**–**5** is the neutral complex $[(^tBuP)_3As]_2$, a principal product of the coupling reaction of $AsCl_3$, $^tBuPCl_2$ and Mg which consists of two $[(^tBuP)_3As]$ rings linked by their As centres.[22] Comparison of the $[(^tBuP)_3As]^-$ ligands of **2**–**4** with $[(^tBuP)_3As]_2$ shows that the effect of concentrating the negative charge on the As centre in these complexes is to decrease the puckering of the P_3As ring unit (the fold angle changing from 36.5° in $[(^tBuP)_3As]_2$ to 27.5° in **2**, 28.1° in **3** and 28° in **4**). This can be attributed mainly to a small change in hybridisation of the As centres, which more closely resembles sp^3 in the $[(^tBuP)_3As]^-$ anion.[23] This view is consistent with the reduction in the As–P bond lengths [mean 2.33 Å in **2**–**4**] and with the increase in the internal P–As–P angles [mean 85.1° in **2**–**4**] compared to those in $[(^tBuP)_3As]_2$ [2.36 Å and 82.56(8)°, respectively]. It is interesting to note also that whereas in **2**–**4** the P–As–Li angles [range 106.4(2)–109.01(9)°] are consistent with sp^3 hybridisation and stereochemically active lone pairs,[23] the more acute internal P–As–P angle in **5** [83.67(4)°] results in a significantly smaller P–As–Li angle (mean 102°).

Complex **6** is obtained exclusively from the same reaction as that producing **1** (Fig. 1), if the temperature is increased to *ca.* 60 °C. The formation of **6** in almost quanititative yield provides a strong indication that the heterocyclic complex **1** is an intermediate in its formation. The low-temperature X-ray study of **6**, which is too thermally unstable to be characterised satisfactorily in the solid state by other means, shows it to be the Zintl compound $[Sb_7Na_3·3TMEDA·3thf]$ (Fig. 6). Although other complexes containing the $[Sb_7]^{3-}$ have been structurally characterised previously,[24] to our knowledge this is the first example where there is an ion-contact between Sb and Na. An interesting feature of this complex is the asymmetrical coordination of the Na^+ cations to the $[Sb_7]^{3-}$ anion. All three Na^+ cations, each

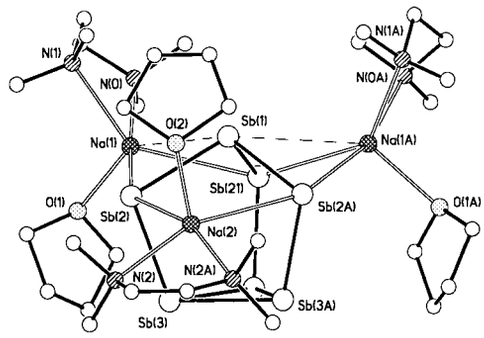

Fig. 6 The structure of the Zintl phase $[Sb_7Na_3·3TMEDA·3thf]$ (**6**), which has crystallographic C_s symmetry, showing the asymmetric coordination of the Na^+ cations. H-atoms are omitted for clarity. Selected bond lengths and angles are listed in Table 3; atom labels ending in A denote atoms at x, $-y + \frac{3}{2}$, z.

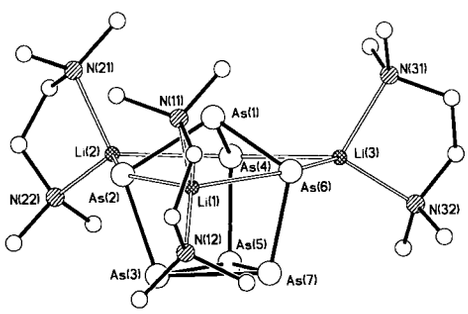

Fig. 7 The structure of the Zintl phase $[As_7Li_3·3TMEDA]·1.5$(toluene) [**7**·1.5(toluene)]. H-atoms and lattice-bound toluene molecules are omitted for clarity. Selected bond lengths and angles are listed in Table 4. Atom labels ending in A denote atoms at $-x$, $-y - 1$, $-z + 1$.

solvated by a thf molecule and by a chelating TMEDA ligand, bond predominantly with the equatorial Sb centres of the $[Sb_7]^{3-}$ anion [the Sb–Na bond lengths (mean Sb–Na 3.25 Å) being similar to the intra-monomer bonds in **1** [3.229(4) Å].[8] However, the two symmetry-related Na^+ cations [Na(1) and Na(1A)] pivot towards and form weak interactions with the apical Sb centre [Sb(1)···Na(1) 3.57(1) Å; *cf.* 3.617(4) Å for the inter-monomer Sb–Na bonds in **1**]. The other Na^+ cation remains five coordinate and the pattern of thf and TMEDA solvation is reversed. The asymmetrical coordination of the three alkali metal cations to the $[Sb_7]^{3-}$ anion in **6** is in contrast to the structures of the Li^+ complexes $[As_7Li_3·TMEDA]$ (**7**) (Fig. 7) and $[Sb_7Li_3·3TMEDA]$,[6] where the alkali metal cations bond exclusively to the equatorial atoms. The most likely explanation for the unusual structural pattern found in **6** lies in the balance between the desire for the larger Na^+ cations to increase their coordination number on one hand, while minimising the resulting steric repulsion between the Lewis base donor ligands on the other. The increase in coordination number of two of the Na^+ cations necessarily results in crowding of the TMEDA ligands in the vicinity of the apical Sb atom of the Zintl ion. Formation of an extra interaction by the third Na^+ cation is therefore unfavourable on steric grounds and by switching the orientation of the thf and TMEDA ligands on this ion steric confrontation with the ligand spheres of the other Na^+ cations is reduced.

Like **6**, $[As_7Li_3·3TMEDA]·1.5$(toluene) [**7**·1.5(toluene)] suffers surface degradation when samples of the complex are isolated under vacuum and, for this reason, elemental analysis was often unsatisfactory. The X-ray structural determination was therefore invaluable in the unequivocal characterisation of the complex. The structure of [**7**·1.5(toluene)] (Fig. 7) is entirely consistent with the earlier preliminary report by Driess and co-workers,[17] the complex being isostructural with the P and Sb analogues $[P_7Li_3·3TMEDA]$[25a] and $[Sb_7Li_3·3TMEDA]$.[6] However, in contrast to the previously reported structure of

unsolvated **7** there is no disordering of the $[As_7Li_3 \cdot 3TMEDA]$ unit and each of the As atoms of the solvate are crystallographically independent (rather than the molecules having C_3 symmetry). Apart from these crystallographic differences, however, the pattern of As–As bond lengths found within the As_7^{3-} anion of **7**·1.5(toluene) is the same as that for the unsolvated complex [*i.e.*, mean As(1)–As(2,4,6) 2.40, mean As(2,4,6)–As(3,5,7) 2.37 and mean As(3,5,7)–As(3,5,7) 2.48 Å; *cf.* 2.427(2), 2.372(2), 2.487(2), respectively, for the corresponding As–As bond lengths in unsolvated **7**[17]]. This pattern is typical of heterosubstituted cluster anions having a nortricyclic structure.[25b]

Conclusions

The general conclusion of this study is that heterocyclic anions of the form $[(RP)_nE]^-$ (E = As, Sb) can be directly accessed from the low-temperature reactions of primary phosphines (REH_2) and metallated primary phosphines (REHM; M = alkali metal) with $E(NMe_2)_3$, if the organic substituents (R) are aliphatic. In the case of aromatic phosphines or arsines direct access to Zintl compounds can be achieved under mild conditions, with no heterocyclic intermediates being isolated.

Experimental

General

Compounds **1**–**8** are air- and moisture-sensitive. They were handled on a vacuum line (in an efficient cupboard) using standard inert atmosphere techniques and under dry/oxygen-free argon.[26] $As(NMe_2)_3$ and $Sb(NMe_2)_3$ were prepared using the literature routes, by transmetallation of $AsCl_3$ and $SbCl_3$ with $LiNMe_2$ (1:3 equiv).[27] They were purified by distillation and stored as standardised solutions in toluene. Thf, toluene, ether and hexane were dried by distillation over sodium–benzophenone prior to the reactions. TMEDA was distilled over CaH_2. The products were isolated and characterized with the aid of an argon-filled glove box fitted with a Belle Technology O_2 and H_2O internal recirculation system. Melting points were determined by using a conventional apparatus and sealing samples in capillaries under argon. IR spectra were recorded as Nujol mulls using NaCl plates and were run on a Perkin-Elmer Paragon 1000 FTIR spectrophotometer. Elemental analyses were performed by first sealing the samples under argon in air-tight aluminium boats (1–2 mg) and C, H and N content was analysed using an Exeter Analytical CE-440 Elemental Analyser. P analysis was carried out by spectrophotometric means. Proton NMR spectra were recorded on a Bruker WM 250 MHz spectrometer in dry deuterated thf (using the solvent resonances as the internal reference standard).

Synthesis of phosphines and arsines[28]

The phosphines $MesPH_2$,[9] $^tBuPH_2$,[10] and 1-$AdPH_2$[11] were prepared using the literature procedures. The synthesis of $MesPH_2$ was based on the procedure by Cowley *et al*. for the synthesis of Mes*PH_2 (Mes* = 2,4,6-$^tBu_3C_6H_2$),[9] typical yields of 80% were obtained for the reduction of $MesPCl_2$ with $LiAlH_4$. The method published by Kostyanovskii *et al*. for the synthesis of $^tBuPH_2$,[10] involving the reduction of $^tBuPCl_2$ with $LiAlH_4$, was modified by using 1,4-dioxane as the solvent (instead of $^tBu_2O$). Yields of *ca.* 60% were obtained by direct distillation of the reaction mixture, without hydrolysis of the $LiAlH_4$.[29] The literature procedure published by Stetter and Last[11] for the synthesis of 1-$AdPH_2$, involving the reaction of 1-AdBr with PCl_3–$AlBr_3$ followed by reduction of 1-$Ad(POCl_2)$ with $LiAlH_4$, was found to be very effective (the yields being 87% and 82%, respectively, for the two steps involved). $PhAsH_2$ was prepared using the method of Palmer and Adams,[12] by the reduction of PhAs(O)OH with Hg–Zn amalgam. It was found that using half the amount of the amalgam as suggested and stirring the mixture for 12 h results in a smoother reaction and consistent yields of 40–60%. $^tBuAsH_2$ was prepared in low yields from the reduction of $^tBuAsCl_2$ with $LiAlH_4$ in Et_2O.[13] The purity of the phosphines and arsines was confirmed by ^1H and ^{31}P NMR spectroscopy.

Since the syntheses of **1** and **2** have been communicated by us previously in reference 8, only the syntheses of the new complexes **3**–**8** are given in detail here.

Synthesis of 3. $^tBuPH_2$ (0.12 ml, 2.0 mmol) in toluene (10 ml) was cooled to 0 °C. $As(NMe_2)_3$ (1.0 ml, 2.0 mmol, 2.0 mol dm^{-3} in toluene) was added dropwise and the mixture warmed to room temperature and stirred (15 min). The resulting solution was added to a suspension of [^tBuPHLi] (2.0 mmol) in toluene (10 ml). Warming to room temperature led to the formation of a yellow precipitate which dissolved on addition of excess TMEDA (1.0 ml, 6.6 mmol). Storage at −20 °C (24 h) gave red crystals of **3**. Yield (0.25 g, 24%). Mp 111 °C. ^1H NMR ([D_8]-thf, 250 MHz, +25 °C), δ 2.40 (s, 12H, -CH_2-, TMEDA), 2.11 (s, 36H, Me_2N-, TMEDA), 1.10 (d, 36H, $^3J_{P\text{-}H}$ = 12 Hz, ^tBu), 1.03 (d, 18H, $^3J_{P\text{-}H}$ = 11 Hz, ^tBu). ^{31}P NMR (100.1 MHz, [D_8]-thf, 101.256 MHz, +25 °C), 7.79 [t, 1P, P(2)], −75.10 [d, 2P, P(1) and P(3)] (J = 181.7 ± 0.8 Hz). Elemental analysis, found C, 48.0; H, 9.7; N, 9.0; P, 16.0; calcd. for [{($^tBuP)_3As$}Li·TMEDA]$_2$·TMEDA C, 48.5; H, 9.8; N, 8.1; P, 17.9%.

Synthesis of 4. To a solution of $^tBuPH_2$ (0.8 ml, 12.0 mmol) in toluene (25 ml) at −78 °C was added ^{n}BuLi (8.0 ml, 1.5 mol dm^{-3} in hexanes, 12.0 mmol). $As(NMe_2)_3$ (1.6 ml, 2.5 mol dm^{-3} in toluene, 4.0 mmol), DABCO (2.67 ml, 1.5 mol dm^{-3}, 4.0 mmol) and thf (5 ml) were added to the suspension of the lithiated phosphine at −78 °C. The mixture was stirred at room temperature (48 h). Filtration, reduction of the orange filtrate under vacuum and storage at room temperature (48 h) gave orange needles of **4**. Yield (0.60g, 23%). ^1H NMR ([D_8]-thf, 250 MHz, +25 °C), 2.55 (s, 18H, ^tBuP), 1.48 (m, 6H, DABCO). ^{31}P NMR (100.1 MHz, [D_8]-thf, 101.256 MHz, +25 °C), 5.0 [t, 1P, P(2)], −73.6 [d, 2P, P(1) and P(3)] (J = 178.1 ± 0.4 Hz). Elemental analysis, found C, 51.2; H, 9.0; N, 9.0; calcd. for [{($^tBuP)_3As$}Li·2DABCO·thf] C, 52.3; H, 9.3; N, 8.7%.

Synthesis of 5. 1-$AdPH_2$ (1.0 ml, 6.0 mmol) in toluene (20 ml) was cooled to −78 °C. ^{n}BuLi (4.0 ml, 1.5 mol dm^{-3} in hexanes, 6.0 mmol) was added. The reaction mixture was allowed to warm to room temperature and was stirred (*ca.* 1 h) to give a yellow precipitate of 1-AdPHLi. $As(NMe_2)_3$ (0.8 ml, 2.5 mol dm^{-3} in toluene, 2.0 mmol) was added to the suspension at −78 °C. Thf (8.0 ml) and excess TMEDA (0.4 ml, 2.65 mmol) were added. The reaction mixture was allowed to warm to room temperature before stirring for a further 12 h. The resulting orange-brown solution was filtered to remove traces of precipitate and the volume was reduced under vacuum until an orange-brown solid precipitated. This was dissolved by gentle heating and the addition of further thf (0.6 ml). Storage at 25 °C (48 h) gave orange-brown crystals of **5**. Yield (0.25 g, 15%). ^1H NMR ([D_8]-thf, 250 MHz, +25 °C), 7.00–7.12 (m, 2.5H, toluene), 3.61 (m, 4H, O–CH_2- of thf), 2.11 (m) and 1.82 (m) (total 45H, 1-Ad groups), 1.54 (m, 4H, -CH_2- thf). ^{31}P NMR (100.1 MHz, [D_8]-thf, 101.256 MHz, +25 °C), −11.87 [t, 1P, P(2)], −89.94 [d, 2P, P(1) and P(3)] (J = 179.0 ± 0.5 Hz). Great difficulty was experienced in obtaining satisfactory C content for the complex. The following results are representative of the results obtained—found C, 61.8; H, 9.0; N, 3.5; calcd. for [{(1-$AdP)_3As$}Li·TMEDA·thf]·0.5(toluene) C, 64.1; H, 9.0; N, 3.4%.

Synthesis of 6. [$Sb(NMe_2)_3$] (10.2 ml, 3.48 mol dm^{-3} in toluene, 17.6 mmol) was added dropwise to a chilled solution of $CyPH_2$ (2.35 ml, 17.6 mmol) in hexane (20 ml). The solution

was allowed to warm to room temperature and stirred (10 min). The orange solution produced was transferred by syringe into a chilled (*ca.* −20 °C) solution of [CyPHNa] (prepared *in situ* by the reaction of $PhCH_2Na$ (2.0 g, 17.6 mmol) with $CyPH_2$ (2.35 ml, 17.6 mmol) in hexane (10 ml)–thf (5 ml). Excess TMEDA (*ca.* 6.0 ml, 40 mmol) was added. The reaction mixture was allowed to warm to *ca.* 25 °C and then briefly heated to reflux. The deep red solution was filtered while warm and storage at −35 °C (24 h) produced a large crop of deep red needle-like crystals. Yield 3.5 g (93% on the basis of the Sb supplied). Although **5** appears to be moderately stable in crystalline form some decomposition always occurs at the surface once isolated under vacuum. As a result satisfactory elemental analysis of **6** could not be obtained.

Synthesis of 7. *Method A*. A suspension of ^{t}BuPHLi (60.0 mmol) in toluene (100 ml) was cooled to 0 °C. $As(NMe_2)_3$ (10.0 ml, 20.0 mmol, 2.0 mol dm^{-3} in toluene) was added dropwise and the mixture warmed to room temperature and stirred (15 min). TMEDA (10.0 ml, 60.0 mmol) was added and the mixture brought to reflux for 48 h. The mixture became orange-red in color as the reaction proceeded. Storage at −20 °C gave yellow crystals of **7**·1.5(toluene). First batch yield (1.0 g, 34%, based on As supplied). Storage of the mother liquor gave further batches of **7**·1.5(toluene) (up to *ca.* 94%). Elemental analysis on **7**·1.5(toluene) was hampered by black surface degradation of crystalline samples once placed under vacuum. Analysis suggests that only one toluene molecule remains after exposure to a vacuum (*ca.* 15 min at 10^{-1} atmospheres): found C, 27.4; H, 5.8; N, 8.4; calcd for **7**·(toluene) C, 26.2; H, 5.2; N, 8.5%.

Method B. $MesPH_2$ (1.0 ml, 6.9 mmol) in Et_2O (15 ml) was cooled to −78 °C and ^{n}BuLi (4.6 ml, 1.5 mol dm^{-3} in hexanes, 6.9 mmol) was added. The reaction mixture was allowed to warm to room temperature and stirred for *ca.* 30 min, affording a yellow precipitate of MesPHLi. The suspension was cooled to −78 °C and $As(NMe_2)_3$ (1.2 ml, 2.0 mol dm^{-3} in toluene, 2.3 mmol) was added dropwise. The reaction mixture was allowed to warm to room temperature and stirred for a further 1 h. Storage at −25 °C gave large yellow cubes of unsolvated **7** (first batch 0.15 g, 51% on the basis of As supplied).

Method C. $PhAsH_2$ (1.0 ml, 8.75 mmol) in toluene (30 ml) was cooled to −78 °C and ^{n}BuLi (5.8 ml 1.5 mol dm^{-3} in hexanes, 8.75 mmol) was added. The reaction mixture was allowed to warm to room temperature and stirred for *ca.* 30 min, affording a yellow precipitate of PhAsHLi. $As(NMe_2)_3$ (1.5 ml, 2.0 mol dm^{-3} in toluene, 2.9 mmol) was added dropwise at −78 °C to this suspension. After addition of thf (10 ml) and TMEDA (0.44 ml), the reaction mixture was allowed to warm to room temperature and stirred for *ca.* 12 h. The volume of the solvent was reduced and a white precipitate was filtered off. Storage at 5 °C gave yellow crystals of **7** [two batches 0.12 g, 28% on the basis of $As(NMe_2)_3$].

The low-temperature X-ray structure of **7**·1.5(toluene) was undertaken on a crystal obtained from Method A. The identities of the products of Methods B and C were confirmed by obtaining the unit cell dimensions of crystalline samples (that for Method B being identical to that previously reported for unsolvated **7**[17] and that from Method C being identical to that from Method A).

Synthesis of 8. To a solution of ^{t}BuAsH$_2$ (0.40 ml, 2.54 mmol) in toluene (10 ml) at −78 °C was added ^{n}BuLi (1.70 ml, 1.6 mol dm^{-3} in hexanes, 2.54 mmol). The reaction mixture was brought to room temperature, giving an orange solution. To this solution at −78 °C was added $As(NMe_2)_3$ (0.34 ml, 2.5 mol dm^{-3} in toluene, 0.86 mmol) and TMEDA (0.13 ml, 0.86 mmol). The orange solid produced redissolved at room temperature. The mixture was allowed to stir at room temperature (1.5 h) and the solvent reduced under vacuum until the product began to precipitate. The precipitate was redissolved by the addition of toluene (1 ml) and thf (1 ml). Storage at room temperature gave **8** as small yellow crystals (*ca.* 0.05 g, 12% on the basis of $As(NMe_2)_3$). The identity of **8** was confirmed by obtaining the unit cell dimensions of the crystals, these being identical with those reported in reference 16.

X-Ray crystallographic studies

Data collection for 3–7. Crystals of **3**, **4**, **5**·0.5(toluene), **6** and **7**·1.5(toluene) were mounted directly from solution under argon using an inert oil which protects them from atmospheric oxygen and moisture.[30] Details of the data collection, refinement and crystal data are listed in Table 1.

Structure solution and refinement for 3–7. In the crystals of both **5** and **7** there was a toluene solvate molecule disordered across an inversion centre, and in **7** there was an additional ordered toluene molecule. In the structure of **6** some disorder of the TMEDA and thf ligands was indicated by relatively high anistropic displacement parameters for the atoms and four carbon atoms were resolved into sites of *ca.* 50 : 50 occupancy. All hydrogen atoms (except those of the disordered toluene molecules of **5** and **7**) were placed in idealised positions. Isotropic displacement parameters were assigned to all hydrogen atoms and set equal to $1.2U_{eq}$ of the parent carbon atoms for the phenyl and methylene groups and $1.5U_{eq}$ for the methyl groups. Semi-empirical absorption corrections using Ψ-scans were applied to the data of **3** and **5**,[31] and after initial refinement with isotropic displacement parameters empirical absorption corrections were applied to the data for **6** and **7**.[32] Chemically equivalent bond lengths involving the disordered ligands in **6**, were constrained to be equal within an esd of 0.02 Å. All non-hydrogen atoms (except in the disordered toluene solvate molecules) were assigned anisotropic displacement parameters in the final cycles of full-matrix least-squares refinement; those of the carbon atoms in the disordered ligands of **6** were constrained to be approximately equal.

CCDC reference number 186/1780.

See http://www.rsc.org/suppdata/dt/a9/a908552a/ for crystallographic files in .cif format.

Acknowledgements

We gratefully acknowledge the EPSRC (A. B., N. C., A. D. H., Y. G. L., M. McP., P. R. R., J. A. W., D. S. W.), the Royal Society (P. R. R., D. S. W.), the Leverhulme Trust (M. A. B.), Electron Industries, Ruislip, UK (A. D. H.), and the EU (Fellowship for M. E. G. M.) for financial support. We also thank Dr J. E. Davies (Cambridge) for collecting X-ray data on **3**–**5**.

References

1 M. A. Beswick, N. Choi, C. N. Harmer, A. D. Hopkins, M. A. Paver, M. McPartlin, P. R. Raithby, A. Steiner, M. Tombul and D. S. Wright, *Inorg. Chem.*, 1998, **37**, 2177.

2 R. Fleischer, S. Freitag, F. Pauer and D. Stalke, *Angew. Chem.*, 1996, **108**, 208; *Angew. Chem., Int. Ed. Engl.*, 1996, **35**, 204; T. Chivers, X. Gao, M. Parvez and G. Schatte, *Inorg. Chem.*, 1996, **35**, 4094.

3 M. A. Beswick and D. S. Wright, *Coord. Chem. Rev.*, 1998, **176**, 373 and references therein.

4 (*a*) M. A. Beswick, C. A. Harmer, M. A. Paver, P. R. Raithby, A. Steiner and D. S. Wright, *Inorg. Chem.*, 1997, **36**, 1740; (*b*) D. Barr, A. J. Edwards, S. Pullen, M. A. Paver, M.-A. Rennie, P. R. Raithby and D. S. Wright, *Angew. Chem.*, 1994, **106**, 1960; *Angew. Chem., Int. Ed. Engl.*, 1994, **33**, 1875; (*c*) A. Bashall, M. A. Beswick, C. N. Harmer, M. A. Paver, M. McPartlin and D. S. Wright, *J. Chem. Soc., Dalton Trans.*, 1998, 517; (*d*) A. Bashall, M. A. Beswick, E. A. Harron, A. D. Hopkins, S. J. Kidd, M. McPartlin, P. R. Raithby, A. Steiner and D. S. Wright, *Chem. Commun.*, 1999, 1145.

5 M. A. Beswick, J. M. Goodman, C. N. Harmer, A. D. Hopkins, M. A. Paver, P. R. Raithby, A. E. H. Wheatley and D. S. Wright, *Chem. Commun.*, 1997, 1897.

6 M. A. Beswick, C. N. Harmer, A. D. Hopkins, M. McPartlin and D. S. Wright, *Science*, 1998, **281**, 1500.
7 A. H. Sommer, *Photoemission Materials*, Kruger, New York, 1968. This approach is a new one, although single-source molecular precursors for the deposition of GaAs from the *vapour* phase have been studied for some time, for example see, (*a*) A. H. Cowley and R. A. Jones, *Angew. Chem.*, 1989, **101**, 1235; *Angew. Chem.*, *Int. Ed. Engl.*, 1989, **28**, 1208; (*b*) R. L. Wells, *Coord. Chem. Rev.*, 1992, 273.
8 M. A. Beswick, N. Choi, A. D. Hopkins, M. E. G. Mosquera, M. McPartlin, P. R. Raithby, A. Rothenberger, D. Stalke, A. E. H. Wheatley and D. S. Wright, *Chem. Commun.*, 1998, 2485.
9 Based on, A. H. Cowley, N. C. Norman and M. Pakulski, *Inorg. Synth.*, **27**, 235.
10 R. G. Kostyanovskii, Y. I. El'natanov, S. M. Shikhaliev, S. M. Ignatov and I. I. Chervin, *Bull. Acad. Sci. USSR Div. Chem. Sci.*, 1982, **31**, 1433.
11 H. Stetter and W. D. Last, *Chem. Ber.*, 1969, **102**, 3364.
12 C. S. Palmer and R. Adams, *J. Am. Chem. Soc.*, 1922, **44**, 356.
13 A. Tzschach and W. Deylig, *Z. Anorg. Allg. Chem.*, 1965, **330**, 317.
14 For example, see J. P. Albrand and C. Taïeb, *Proceedings of the 1981 International Conference on Phosphorus Chemistry*, ACS Symposium Series, 1981, ch. 119, 577.
15 (*a*) E. D. Becker, *High Resolution NMR*; *Theory and Chemical Applications*, 2nd edn., Academic Press, New York, 1980, p. 167; (*b*) M. Baudler, G. Reuschenbach, J. Hellmann and J. Hahn, *Z. Anorg. Allg. Chem.*, 1983, **499**, 89; (*c*) *Panic- Parameter Adjustment in NMR by Iterative Calculation*, Aspect 2000/3000 NMR software, version 85050, Bruker, 1986.
16 C. v. Hanisch and D. Fenske, *Z. Anorg. Allg. Chem.*, 1997, **623**, 1040.
17 M. Driess, K. Metz, H. Pritzkow and R. Janoschek, *Angew. Chem.*, 1996, **106**, 2688; *Angew. Chem.*, *Int. Ed. Engl.*, 1996, **35**, 2507.
18 B. Tecle, W. H. Isley and J. P. Oliver, *Organometallics*, 1982, **1**, 875.
19 S. Harder, J. Boersma, L. Brandsma and J. A. Kanters, *J. Organomet. Chem.*, 1988, **339**, 7; M. P. Bernstein, P. E. Romesberg, O. J. Fuller, A. T. Harrison, D. B. Collum, Q. Y. Lui and P. G. Williard, *J. Am. Chem. Soc.*, 1992, **114**, 5100; W. A. Nichols and P. G. Williard, *J. Am. Chem. Soc.*, 1993, **115**, 1568; K. Tatsnai, Y. Inone, H. Kawaguchi, M. Kohsaka, A. Nahamura, R. E. Cramer, W. Van Doome, G. T. Taogoshi and P. N. Richmann, *Organometallics*, 1993, **12**, 352; D. Hoffman, A. Dorigo, P. v. R. Schleyer, H. Reif, D. Stalke, G. M. Sheldrick, E. Weiss and M. Geissler, *Inorg. Chem.*, 1995, **34**, 262.
20 (*a*) H. Schumann and E. Palamidis, *Organometallics*, 1982, **7**, 1008; (*b*) G. Becker and C. Whitthauer, *Z. Anorg. Allg. Chem.*, 1982, **492**, 28; (*c*) A. M. Arif, R. A. Jones and K. B. Kidd, *J. Chem. Soc.*, *Chem. Commun.*, 1986, 1440; (*d*) R. A. Barlett, H. V. R. Dias, H. Hope, D. D. Murray, M. M. Olmstead and P. P. Power, *J. Am. Chem. Soc.*, 1986, **108**, 6921; (*e*) M. Driess and H. Pritzkow, *Angew. Chem.*, 1992, **104**, 350; *Angew. Chem.*, *Int. Ed. Engl.*, 1992, **31**, 316; (*f*) L. Zsolnai, G. Huttner and M. Driess, *Angew. Chem.*, 1993, **105**, 1549; *Angew. Chem.*, *Int. Ed. Engl.*, 1993, **32**, 1439; (*g*) M. Driess, H. Pritzkow, S. Martin, S. Rell, D. Fenske and G. Baum, *Angew. Chem.*, 1996, **108**, 1064; *Angew. Chem.*, *Int. Ed. Engl.*, 1996, **35**, 986.
21 For examples, (*a*) L. W. Weber, D. Bungardt and R. Boese, *Z. Anorg. Allg. Chem.*, 1989, **578**, 205; (*b*) A. L. Rheingold and F. P. Arnold, *Inorg. Chim. Acta*, 1992, **298**, 139.
22 H. Baudler, Y. Aktalay, T. Heinlein and K. F. Tebbe, *Z. Naturforsch.*, *Teil B*, 1982, **37**, 299.
23 H. A. Bent, *J. Chem. Educ.*, 1960, **37**, 616; *J. Chem. Phys.*, 1960, **33**, 1258; *Chem. Rev.*, 1961, **61**, 275.
24 J. D. Corbett, *Chem. Rev.*, 1985, **85**, 383; H. G. von Schnering, *Angew. Chem.*, 1981, **93**, 44; *Angew. Chem.*, *Int. Ed. Engl.*, 1981, **20**, 33, and references therein.
25 (*a*) W. Hönle, H. G. von Schnering, A. Schmidpeter and G. Burget, *Angew. Chem.*, 1984, **96**, 796; *Angew. Chem.*, *Int. Ed. Engl.*, 1984, **23**, 817; (*b*) W. Schmettow and H. G. von Schnering, *Angew. Chem.*, 1977, **89**, 895; *Angew. Chem.*, *Int. Ed. Engl.*, 1977, **16**, 857.
26 D. F. Shriver and M. A. Drezdon, *The Manipulation of Air-Sensitive Compounds*, 2nd edn., Wiley, New York, 1986.
27 K. Moedritzer, *Inorg. Chem.*, 1964, **3**, 609; F. Ando, T. Hayashi, K. Ohashi and J. Kotetsu, *J. Nucl. Chem.*, 1991, **30**, 2011.
28 **Health and Safety Warning**: All these materials (and the precursor halides) are highly toxic and air-sensitive. $^{t}BuPH_2$ is pyrophoric and should never be allowed to come into contact with combustible material (*e.g.*, paper). $PhAsH_2$ and $^{t}BuAsH_2$ cause serious skin burns and respiratory difficulty. They should be handled with extreme care in an efficient fume cupboard.
29 Great care should be taken to ensure that the reduction of $^{t}BuPCl_2$ with $LiAlH_4$ is initiated before complete addition of the dihalide. In a typical preparation, a solution of $^{t}BuPCl_2$ (56 g, 0.35 mol) in 1,4-dioxane is added dropwise to a suspension of $LiAlH_4$ in 1,4-dioxane (30 g, 0.79 mol) at room temperature with vigorous stirring. The reaction should initiate after addition of a few dm^3 of the $^{t}BuPCl_2$ solution (gentle heating may be required). The reaction is stirred at room temperature overnight before fractional distillation with a 10 inch vigreaux column (60–80 °C).
30 T. Kottke and D. Stalke, *J. Appl. Crystallogr.*, 1993, **26**, 615.
31 SHELXTL PC version 5.03, Siemens Analytical Instruments, Madison, WI, 1994.
32 N. Walker and D. Stuart, *Acta Crystallogr.*, *Sect. A*, 1983, **39**, 158.

Paper a908552a